THE JOURNAL OF BIOLOGICAL CHEMISTRY VOL. 285, NO. 11, pp. 8278–8289, March 12, 2010

Sucrose Octasulfate Selectively Accelerates Thrombin Inactivation by Heparin Cofactor II*

Received for publication, April 8, 2009, and in revised form, December 23, 2009 Published, JBC Papers in Press, January 6, 2010, DOI 10.1074/jbc.M109.005967

Suryakala Sarilla, Sally Y. Habib, Dmitri V. Kravtsov, Anton Matafonov, David Gailani, and Ingrid M. Verhamme[1]

From the Department of Pathology, Vanderbilt University School of Medicine, Nashville, Tennessee 37232

Inactivation of thrombin (T) by the serpins heparin cofactor II (HCII) and antithrombin (AT) is accelerated by a heparin template between the serpin and thrombin exosite II. Unlike AT, HCII also uses an allosteric interaction of its NH_2-terminal segment with exosite I. Sucrose octasulfate (SOS) accelerated thrombin inactivation by HCII but not AT by 2000-fold. SOS bound to two sites on thrombin, with dissociation constants (K_D) of 10 ± 4 μM and 400 ± 300 μM that were not kinetically resolvable, as evidenced by single hyperbolic SOS concentration dependences of the inactivation rate (k_{obs}). SOS bound HCII with K_D 1.45 ± 0.30 mM, and this binding was tightened in the T·SOS·HCII complex, characterized by $K_{complex}$ of ~0.20 μM. Inactivation data were incompatible with a model solely depending on HCII·SOS but fit an equilibrium linkage model employing T·SOS binding in the pathway to higher order complex formation. Hirudin-(54–65)(SO_3^-) caused a hyperbolic decrease of the inactivation rates, suggesting partial competitive binding of hirudin-(54–65)(SO_3^-) and HCII to exosite I. Meizothrombin(des-fragment 1), binding SOS with K_D = 1600 ± 300 μM, and thrombin were inactivated at comparable rates, and an exosite II aptamer had no effect on the inactivation, suggesting limited exosite II involvement. SOS accelerated inactivation of meizothrombin 1000-fold, reflecting the contribution of direct exosite I interaction with HCII. Thrombin generation in plasma was suppressed by SOS, both in HCII-dependent and -independent processes. The *ex vivo* HCII-dependent process may utilize the proposed model and suggests a potential for oversulfated disaccharides in controlling HCII-regulated thrombin generation.

The central coagulation proteinase, α-thrombin (T),[2] is covalently inactivated by the serpins antithrombin (AT) and heparin cofactor II (HCII), in reactions that are accelerated by sulfated glycosaminoglycans (GAGs) (1–6). Two electropositive sites on thrombin, exosites I and II, are differentially involved in its inactivation by HCII and AT (7, 8). High molecular weight GAGs act as templates between thrombin exosite II and the GAG binding sites on AT and HCII (1, 2, 5, 9–11), and an 18 saccharide unit length is required for template activity (12).

The HCII mechanism also utilizes the allosteric interaction of thrombin exosite I with the Glu^{53}–Asp^{75} acidic sequence in the HCII NH_2-terminal region that contains two hirudin-(54–65)-like repeats (3, 4, 13–17). This sequence, not present in AT, becomes available for thrombin interaction upon GAG binding of HCII (3, 16). Direct evidence was provided by the crystal structure of the HCII·S195A-thrombin Michaelis complex, in which residues 56–72 of HCII make contact with exosite I (16). Both repeats are required for heparin- and DS-catalyzed thrombin inactivation, as demonstrated by the decreased inhibitory potential of HCII NH_2-terminal deletion mutants (3, 14). Mutation of thrombin exosite I residues Arg^{67} and Arg^{73} resulted in significantly slower inactivation by native HCII (15).

In reactions utilizing template-forming GAGs, both the template and allosteric interactions contribute to the mechanism by binding of GAG to thrombin exosite II and interaction of thrombin-complexed GAG with the heparin binding site in HCII, thereby triggering interaction of the HCII NH_2-terminal sequence with exosite I. The intermediate T·GAG·HCII complexes, stabilized by two interactions, are significantly tighter than the T·GAG·AT complexes (9).

Oligosaccharides shorter than 18 saccharide units, such as dermatan sulfate hexasaccharides, and sulfated bis-lactobionic and bis-maltobionic acid amides moderately accelerated inhibition by HCII but not AT (18–20). These molecules are too small for template action, and it is unknown whether they bind to thrombin. Their mechanism of action is proposed to be solely allosteric, by binding to HCII and triggering interaction of the NH_2-terminal sequence with exosite I. The sulfated disaccharide, sucrose octasulfate (SOS), a known anti-ulcer drug (21) recently identified as an antitumor agent (22), exhibits moderate anticoagulant properties, measured by clotting assays (22, 23). The present work describes the ~2000-fold accelerating effect of SOS on the inactivation of thrombin by HCII, demonstrates the involvement of thrombin exosite I, and

* This work was supported, in whole or in part, by National Institutes of Health, NHLBI, Grants RO1 HL 080018 (to I. M. V.) and RO1 HL058837 (to D. G.).

[1] To whom correspondence should be addressed: C3321A Medical Center North, Nashville, TN 37232-2561. Tel.: 615-343-6563; Fax: 615-343-7023; E-mail: ingrid.verhamme@vanderbilt.edu.

[2] The abbreviations and trivial names used are: T, human α-thrombin; AT, antithrombin; HCII, heparin cofactor II; fXa, human factor Xa; TF, tissue factor; GAG, glycosaminoglycan; DS, dermatan sulfate; TNS, 2-(*p*-toluidinyl)naphthalene-6-sulfonic acid; [ANS]FPR-T, [2-((4′-acetamido)anilino)-naphthalene-6-sulfonic acid]-D-Phe-Pro-Arg-thrombin; MzT, meizothrombin; Mz(-F1), meizothrombin(des-fragment 1); [ANS]FPR-Mz(-F1), [2-((4′-acetamido)anilino)naphthalene-6-sulfonic acid]-D-Phe-Pro-Arg-Mz(-F1); Hir-(54–65)(SO_3^-), Gly-Asp-Phe-Glu-Glu-Ile-Pro-Glu-Glu-Tyr(SO_3^-)-Leu-Gln; [5F]Hir-(54–65)(SO_3^-), Hir-(54–65)(SO_3^-) labeled at the NH_2 terminus with 5-carboxy(fluorescein); S2238, H-D-Phe-Pip-Arg-*p*-nitroanilide; CBS31.39, CH_3SO_2-D-Leu-Gly-Arg-*p*-nitroanilide; Chromozym TH, Tos-Gly-Pro-Arg-*p*-nitroanilide; Spectrozyme fXa, methoxycarbonyl-*D*-cyclohexylglycyl-Gly-Arg-*p*-nitroanilide; *p*NA, *p*-nitroaniline; CAT, calibrated automated thrombography; PNP, pooled human normal plasma; SOS, sucrose octasulfate; ETP, endogenous thrombin potential.

proposes a mechanism in which both the enzyme and the serpin, complexed with SOS, associate in higher order complexes preceding covalent thrombin inactivation. Combined analysis of equilibrium binding and kinetic data demonstrated substantial tightening of HCII binding in the higher order complexes. SOS did not increase the rate of thrombin inactivation by AT, although it bound to its heparin binding site. The studies support a linked equilibrium mechanism in which SOS-bound thrombin reacts with HCII and HCII·SOS complexes to trigger allosteric interaction. SOS suppressed *ex vivo* thrombin generation in human plasma both in an HCII-dependent and -independent process, the latter possibly involving inhibition of prothrombin activation. The data suggest the potential of novel, highly sulfated disaccharide therapeutic agents based on the structure of SOS in regulating thrombin generation and activity.

EXPERIMENTAL PROCEDURES

Proteins and Materials—Human HCII, AT, factor V, and prothrombin were purified from plasma (9, 24–26), and α-thrombin, factor Xa (fXa), and factor Va were prepared as described (25–27). Human R155A,R271A,R284A and R271A,R284A prothrombin variants were expressed in AD293 cells, purified as described, and activated to meizothrombin (MzT) and meizothrombin(des-fragment 1) (Mz(-F1)) with ecarin (28). Protein concentrations were determined by absorbance at 280 nm with the absorption coefficients and molecular weights (M_r) of 1.83 $(mg/ml)^{-1}$ cm^{-1} and 36,700, respectively, for thrombin (29); 1.44 and 72,000 for prothrombin and meizothrombin (30); 1.78 and 49,900 for Mz(-F1) (31); 1.16 and 46,000 for factor Xa (27); 0.89 and 330,000 for factor Va (26); 0.59 and 65,600 for HCII (32); and 0.65 and 58,000 for AT (24). Active HCII and AT concentrations were determined by stoichiometric titration with thrombin. SOS (Toronto Research Chemicals), sheep and goat anti-human HCII antibodies (Affinity Biologicals, Hematologic Technologies), human pooled normal plasma (PNP) (George King Bio-Medical Inc.), HCII-immunodepleted plasma (Affinity Biologicals, Innovative Research), porcine intestinal mucosa DS (Celsus), egg yolk phosphatidylcholine and porcine brain phosphatidylserine (Avanti Polar Lipids), recombinant human tissue factor (TF) (Dade Behring), fondaparinux (GlaxoSmithKline), hirudin peptide (Hir-(54–65)(SO_3^-)), exosite II aptamer HD-22 (Midland), and corn trypsin inhibitor (Sigma) were purchased. Chromogenic substrates S2238, Chromozym TH, CBS31.39, and Spectrozyme fXa were from Chromogenix, Roche Applied Science, Stago, and American Diagnostica. The fluorescence labels TNS and 2-((4′-iodo-acetamido)anilino)-naphthalene-6-sulfonic acid were from Molecular Probes. The fluorogenic substrate benzyloxycarbonyl-GGR-amido-4-methylcoumarin and thrombin calibrator were from Thrombinoscope BV (Maastricht, The Netherlands). Fluorescein-labeled hirudin peptide ([5F]Hir-(54–65)(SO_3^-)) (33) and 2-((4′-acetamido)-anilino)naphthalene-6-sulfonic acid active site-labeled thrombin ([ANS]FPR-T) and Mz(-F1) ([ANS]FPR-Mz(-F1)) were prepared as described (25, 27). DS was treated with nitrous acid to remove heparin (20). Experiments were performed under thermostated conditions at 25 °C in 50 mM Hepes, 0.11 M NaCl, 5 mM $CaCl_2$, 1 mg/ml polyethylene glycol 8000, pH 7.4, buffer.

Fluorescence Equilibrium Binding of SOS to Thrombin, Mz(-F1), HCII, and AT—Fluorescence titrations were performed as described (34) with an SLM 8100 spectrofluorometer equipped with an Olis photon counter ([ANS]FPR-T and [ANS]FPR-Mz(-F1)) or in the ratio mode (serpin·TNS), using acrylic cuvettes coated with polyethylene glycol 20,000 to minimize protein adsorption. Excitation and emission wavelengths were 332 and 446 nm for SOS binding to [ANS]FPR-T and [ANS]FPR-Mz(-F1) and 330 and 428 nm for binding to the serpin·TNS complexes. Band passes were 4–8 nm. Titration curves were obtained from multiple cuvettes with overlapping SOS concentrations, with six additions per cuvette. Corrections were made for probe drift caused by mixing and dilution and for TNS and SOS background. Results were expressed as the fractional change in the initial fluorescence ($(F_o - F_o)/F_o = \Delta F/F_o$) as a function of total SOS concentration.

SOS binding to HCII (500 nM) and AT (3.7 and 4.5 μM) was quantitated by the change in fluorescence of the reversible probe TNS (12 μM) in the serpin·TNS complex upon binding of SOS (35, 36). Data were analyzed by the quadratic equation for binding of a single ligand (27) to obtain the maximum fluorescence intensity changes $\Delta F_{max,HCII(SOS)}/F_o$ and $\Delta F_{max,AT(SOS)}/F_o$ and the dissociation constants $K_{HCII(SOS)}$ and $K_{AT(SOS)}$, with one binding site for SOS assumed on HCII or AT ($n = 1$).

Titrations of SOS binding to [ANS]FPR-T (169 and 390 nM) were analyzed by Equation 1 for two binding sites under first-order conditions,

$$\frac{\Delta F}{F_o} = \frac{F_{lim,T(SOS)} \cdot [SOS]_o}{K_{T(SOS)} + [SOS]_o} + \frac{F_{lim,T(SOS)2} \cdot [SOS]_o}{K_{T(SOS)2} + [SOS]_o} \qquad \text{(Eq. 1)}$$

with the fitted dissociation constants $K_{T(SOS)}$ and $K_{T(SOS)_2}$ and with $F_{lim,T(SOS)}$ and $F_{lim,T(SOS)_2}$ representing the amplitudes for T·SOS and T·$(SOS)_2$ formation. Goodness of fit of the two-binding site model was compared with alternative binding models for a single binding site and single binding combined with nonspecific fluorescence change (34), using the extra sum-of-squares F test. SOS binding to [ANS]FPR-Mz(-F1) (343 nM) was analyzed by the model for binding of a single ligand (27).

Kinetics of SOS-accelerated Enzyme Inactivation by HCII—Thrombin, MzT, and Mz(-F1) inactivation was measured by continuous competitive chromogenic substrate hydrolysis (9, 37, 38). K_m and k_{cat} for hydrolysis of S2238 and Chromozym TH were 1.5 μM and 90 s^{-1} (39), and 11 μM and 167 s^{-1}, respectively, determined from progress curve analysis of *p*NA formation at 405 nm (40). K_m and k_{cat} for hydrolysis of CBS31.39 were 240 ± 20 μM and 49 ± 1 s^{-1} from the Michaelis-Menten concentration dependence of the initial rates of *p*NA formation. Kinetic parameters for substrate hydrolysis by MzT and Mz(-F1) were not significantly different (30). SOS, at the highest experimental concentrations (2.5 mM), had no effect on the hydrolysis of S2238 and Chromozym TH and ≤10% effect on the rate of hydrolysis of CBS31.39. Control reactions using 20 mM free sulfate instead of SOS demonstrated the absence of nonspecific ionic effects. Higher SOS concentrations were not

used in the kinetics to avoid effects caused by the ionic contribution of SOS.

Inactivation reactions were first-order with respect to HCII, SOS, and chromogenic substrate, and less than 20% of the substrate was consumed. Time courses were analyzed by nonlinear least squares fitting by Equations 2–4,

$$[pNA]_t = A\cdot(1 - \exp^{-k_{obs}t}) + X \quad \text{(Eq. 2)}$$

$$k_{obs} = \frac{k}{1 + \frac{[S]_o}{K_m}} \quad \text{(Eq. 3)}$$

$$k = k'\cdot[HCII]_o \quad \text{(Eq. 4)}$$

where $[pNA]_t$ represents the concentration of *p*NA formed at time *t*, $[S]_o$ and $[HCII]_o$ are the initial substrate and HCII concentrations, *A* is the amplitude of the progress curve, K_m is the Michaelis constant of substrate hydrolysis, k_{obs} and *k* are the pseudo-first-order rate constants in the presence and absence of competing substrate, and *k′* is the second-order inactivation rate constant. A second exponential *X* accounted for the combined effects of trace γ-thrombin (4), the uncatalyzed component of enzyme reacting with HCII, and other forms of slowly reacting enzyme (41, 42).

SOS and HCII dependences of k_{obs} were established at various fixed concentrations of HCII and SOS, respectively, and 150–200 μM Chromozym TH, CBS31.39, or S2238. Enzyme concentrations were typically 0.5–5 nM in reactions with Chromozym TH and S2238 and 10–30 nM in reactions with CBS31.39. The SOS and HCII dependences of k_{obs} were fit by Equation 5 (1, 9),

$$k_{obs} = \frac{k_{lim}[HCII]_o/(1 + [S]_o/K_m)}{K_{complex}(1 + K_{T(SOS)_{app}}/[SOS]_{free}) + [HCII]_o/(1 + [S]_o/K_m)} \quad \text{(Eq. 5)}$$

where k_{lim} represents the limiting maximal first-order rate constant, $K_{T(SOS)app}$ is the apparent K_D for overall binding of SOS to thrombin, and $K_{complex}$ is the overall apparent Michaelis constant for assembly of the T·SOS·HCII and T·SOS·HCII·SOS complexes. Under the experimental conditions, $[SOS]_o \gg [T]_o + [HCII]_o$, and $[SOS]_{free} \cong [SOS]_o$. The independent variable $[HCII]_o$ was divided by the competitive factor for chromogenic substrate ($[HCII]_o/(1 + [S]_o/K_m)$) (9, 25, 43). This approach allowed the combination of data obtained with different substrates into one data array, using $[HCII]_o$ concentrations up to 10 μM. Data were also fit by a hyperbolic HCII·SOS dependence that did not take into account SOS binding to thrombin and equilibrium linkage in ternary complex formation (44), using the independent variable $[HCII\cdot SOS]/(1 + [S]_o/K_m)$ and omitting the factor $(1 + K_{T(SOS)app}/[SOS]_{free})$ that defines SOS binding to thrombin and equilibrium linkage.

SOS dependences of the apparent second-order rate constant *k′* were fit by Equation 6,

$$k' = \frac{k'_{lim}[SOS]_o}{K_{app} + [SOS]_o} + k'_{uncat} \quad \text{(Eq. 6)}$$

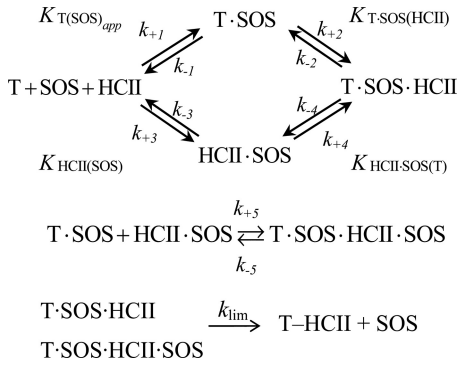

SCHEME 1. **Individual pathway contributions to formation of higher order reversible complexes preceding covalent inactivation.**

where k'_{lim} represents the maximal value of *k′* at saturating SOS, K_{app} is the apparent K_D for overall SOS binding in the complex, and k'_{uncat} is the rate constant in the absence of SOS. Dependences of Mz(-F1) and MzT inactivation were analyzed similarly.

Individual pathway contributions to formation of higher order reversible complexes preceding covalent inactivation were calculated by numerical integration using the equations in Scheme 1, using Kintek Global Kinetic Explorer (45, 46). Dissociation constants were considered near rapid equilibrium, and fixed forward rate constants of 32 $\mu M^{-1}\ s^{-1}$ were used in the integration, consistent with the association rate constant for binding of pentasaccharide to AT at 0.15 M ionic strength (47). $K_{complex}$ represented both $K_{TSOS(HCII)} = k_{-2}/k_{+2}$, governing formation of T·SOS·HCII complex, and k_{-5}/k_{+5}, governing formation of T·SOS·HCII·SOS. $K_{HCII\cdot SOS(T)} = k_{-4}/k_{+4}$ was calculated from detailed balance $k_{-1}k_{-1}/k_{+1}k_{+2} = k_{-3}k_{-4}/k_{+3}k_{+4}$. Formation of covalent T-HCII complex from T·SOS·HCII and T·SOS·HCII·SOS was dictated by the limiting rate k_{lim} from the inactivation kinetics.

Specificity of SOS for the Thrombin-HCII Interaction—The effect of SOS on thrombin inactivation by AT was measured from the loss of thrombin activity under pseudo-first-order conditions (500 nM $[AT]_o$, 50 nM $[T]_o$), at 0, 50, and 500 μM SOS. Residual thrombin activity ($[T]_t$) was measured at discrete time intervals and expressed as the fraction of the initial activity ($[T]_o$). Time courses of the fractional residual thrombin activity were analyzed by the first-order equation, $[T]_t/[T]_o = e^{-kt}$, with $k = k'\cdot[AT]_o$, the product of the second-order rate constant for the T-AT reaction and the AT concentration.

Inactivation of fXa (0.6 nM) by AT (65 nM), accelerated by the AT-specific pentasaccharide fondaparinux (500 nM), was measured at 0, 200, and 2000 μM SOS and 160 μM Spectrozyme fXa. Under these conditions, SOS had a negligible effect on the fXa-AT reaction in the absence of fondaparinux. Progress curves were analyzed using K_m and k_{cat} for hydrolysis of Spectrozyme fXa by fXa of 98 μM and 172 s^{-1} (48).

Role of Exosite I in the SOS-accelerated T-HCII Reaction—Equilibrium binding titrations of 29 nM fluorescein-labeled hirudin peptide ([5F]Hir-(54–65)(SO_3^-)) with thrombin were performed in the absence and presence of 518 μM SOS. Binding was analyzed by the quadratic equation for binding of a single ligand (27) to obtain $\Delta F_{max,T(Hir)}/F_o$ and $K_{T(Hir)}$ in the absence

and presence of SOS, assuming one binding site for [5F]Hir-(54–65)(SO_3^-) on exosite I. Thrombin inactivation was measured at increasing Hir-(54–65)(SO_3^-) concentrations, at 27 nM thrombin, 166 nM HCII, 150 μM CBS31.39, and 518 μM SOS. The Hir-(54–65)(SO_3^-) dependence of k_{obs} was fit by Equation 7, describing binding of Hir-(54–65)(SO_3^-) to SOS-complexed thrombin during its inactivation by HCII, with no assumptions as to whether binding of Hir-(54–65)(SO_3^-) and the HCII NH_2-terminal segment on thrombin exosite I is mutually exclusive or overlapping.

$$k_{obs} = k_i'[HCII]_o + (k'_{T\cdot SOS(Hir)} - k_i')[HCII]_o\left(\frac{[T\cdot SOS\cdot Hir]_o}{[T\cdot SOS]_o}\right) \quad \text{(Eq. 7)}$$

The fraction of SOS-complexed thrombin bound to peptide, $[T\cdot SOS\cdot Hir]_o/[T]_o$, is defined by the quadratic binding equations for peptide binding to thrombin. The second-order rate constants for T·SOS and the T·SOS·Hir complex reacting with HCII are k_i' and $k'_{T\cdot SOS(Hir)}$ (33, 34). The results were compared with a model for mutually exclusive binding of Hir-(54–65)(SO_3^-) and the HCII NH_2-terminal segment to thrombin exosite I (49).

Role of Exosite II in the SOS-accelerated T-HCII Reaction—The role of exosite II was evaluated by measuring inactivation of R155A,R271A,R284A MzT and R271A,R284A Mz(-F1). Inactivation reactions were performed with 1–5 nM enzyme, 0.17–6 μM HCII, 119–157 μM Chromozym TH, and 50–2000 μM SOS. The effect of 1.2 μM exosite II aptamer HD-22 (50) was measured on thrombin inactivation by HCII (166 nM) at 500 μM SOS. Least squares fitting of binding and kinetic data were performed with SCIENTIST (MicroMath) or GraphPad Prism. Errors represent ±2 S.D.

Thrombin Generation in Normal (PNP) and HCII-immunodepleted Plasma—Thrombin generation in human PNP and HCII-immunodepleted plasma was measured at 37 °C by monitoring the conversion of the fluorogenic substrate benzyloxycarbonyl-GGR-amido-4-methylcoumarin, using a Spectramax M2 fluorescence microplate reader (Synapse BV, Maastricht, The Netherlands) with 390-nm excitation and 460-nm emission filters. HCII-immunodepleted plasma tested negative for HCII by Western blot analysis. Plasma was treated with 70 μM corn trypsin inhibitor to block activation of the intrinsic pathway (51), and fluorogenic substrate was added to a concentration of 416 μM in the final reaction mixture. The plasma mixture (80 μl) was added to 20 μl of a mixture containing 80:20 phosphatidylcholine/phosphatidylserine (5 μM final), a trigger, and SOS (0–5 mM final) in Tyrode's buffer (137 mM NaCl, 2.8 mM KCl, 12 mM $NaHCO_3$, 5.5 mM glucose, 0.4 mM NaH_2PO_4, and 10 mM Hepes, pH 7.4). Controls in immunodepleted plasma contained 0–5 μM heparin-free DS. Trigger was either recombinant human TF (16 pM final) or human fXa (3 nM final). After incubation at 37 °C, the reaction was initiated by the addition of 20 μl of a $CaCl_2$ solution (17 mM final) in 20 mM HEPES buffer, pH 7.4, 37 °C, containing bovine serum albumin (10 mg/ml final). In separate experiments, polyclonal sheep and goat anti-human HCII antibodies were used to inactivate HCII in normal plasma in reactions containing 1, 2, or 5 mM SOS. Small volumes (8 μl) of concentrated antibody or Tyrode's buffer control were included in the 80-μl plasma/reagent mixture to a final concentration of 9 μM antibody, followed by incubation and reaction initiation with $CaCl_2$. Thrombin generation was calibrated using α_2-macroglobulin-caged thrombin to correct for inner filter effects and substrate consumption. Each plasma batch required its own calibrator readings due to individual plasma color effects on the fluorescence of the product. Calibrator concentration was adjusted to measure maximal generated thrombin activity of 600 nM. Wells containing calibrator (20 μl) together with the plasma-fluorogenic substrate mixture in the absence of trigger were supplemented with $CaCl_2$ solution in parallel with the assay wells. In control experiments, 5 mM SOS had no effect on calibrator activity. Thrombin generation (nM), and the endogenous thrombin potential (ETP) (nM), represented by the area under the curve, were analyzed with Thrombinoscope software (52, 53). The dependences of the observed ETP (ETP_{obs}) on the total SOS concentration were analyzed by Equation 8,

$$ETP_{obs} = \frac{(ETP_{lim} - ETP_o)[SOS]_o}{A + [SOS]_o} + ETP_o \quad \text{(Eq. 8)}$$

where ETP_{lim} represents the limiting ETP value at saturating SOS, ETP_o is the value in the absence of SOS, and A is the SOS concentration at which a 50% decrease of the ETP is observed.

Effect of SOS on in Vitro Prothrombin Activation—Plasma prothrombin (50 nM) was incubated with 10 nM factor Va, 60 μM 80:20 phosphatidylcholine/phosphatidylserine, and 140 μM S2238 in reaction buffer, pH 7.4, at 25 °C, and the reaction was started by adding 7 pM fXa. Thrombin generation was measured continuously for 2 min in the absence and presence of 600 μM SOS.

RESULTS

Fluorescence Equilibrium Binding of SOS to HCII, AT, and Thrombin—SOS binding to HCII·TNS and AT·TNS was measured, using a method specifically reporting GAG binding to the heparin-binding sites in both serpins (35, 36). The binding analysis gave $K_{HCII(SOS)} = 1.45 \pm 0.30$ mM (Fig. 1*A*) and $K_{AT(SOS)} = 90 \pm 10$ μM (Fig. 1*B*), with one binding site for SOS assumed on HCII or AT. SOS binding to HCII was ~17-fold weaker than binding to AT.

Parameters for SOS binding to [ANS]FPR-T, analyzed by the equation for binding of a single ligand, or a single specific ligand with a nonspecific binding term are given in Table 1, with the fitted curves shown as *dashed lines* in Fig. 2*A*. These analyses showed a distinct nonrandom residual distribution, and the data were fit by Equation 1 for binding of two ligands. The fitted parameters were $K_{T(SOS)} = 10 \pm 4$ μM and $K_{T(SOS)_2} = 400 \pm 300$ μM, with similar amplitudes (Table 1). The extra sum of squares F test indicated that the two-site model was superior to the single-site model ($F = 35.8$ and $p < 0.0001$) and the single-site model with a nonspecific component ($F = 44.4$ and $p < 0.0001$). Binding of SOS to [ANS]FPR-Mz(-F1) was characterized by $K_{Mz(-F1)(SOS)} = 1600 \pm 500$ μM and $\Delta F_{max}/F_o = -36 \pm 6\%$ for binding of a single ligand (Fig. 2*B*).

Binding of SOS to HCII and thrombin did not cause a change in protein tryptophan fluorescence, and SOS binding to thrombin had only a small, ≤10% effect on the hydrolysis of CBS31.39.

Thrombin-HCII Inactivation Kinetics—An array of progress curves for thrombin inactivation by HCII in the presence of Chromozym TH, at increasing SOS concentrations, and a control reaction with free sulfate are shown in Fig. 3*A*. The hyperbolic HCII and SOS concentration dependences of k_{obs} (Figs. 3*B* and 4*A*) were fit by Equation 5. Rate constants at experimentally limiting HCII and SOS concentrations of 10 and 2500 μM, respectively, were instrumental in determining the constraints for the limiting rate k_{lim}. Global fitting of both HCII and SOS dependences yielded 200 ± 100 μM for $K_{T(SOS)app}$, the apparent binding constant for overall binding of SOS to thrombin; 0.12 ± 0.04 μM for $K_{complex}$, the apparent Michaelis constant for T·SOS binding to free or SOS-complexed HCII; and 0.12 ± 0.02 s^{-1} for k_{lim}. The dissociation constant $K_{HCII(SOS)}$ for SOS binding was fixed at 1.45 mM, obtained independently by equilibrium binding. Fitting the HCII data set separately gave similar parameters (Table 1). The ratio $k_{lim}/K_{complex}$ represents the second-order rate constant in the presence of SOS, ~2000-fold faster than that observed in the uncatalyzed reaction. The $K_{complex}$ dissociation constant reflects the tightening of HCII binding in the higher order complexes and is the theoretical effective HCII concentration at half-saturation of the HCII dependence of k_{obs} (Fig. 3*B*). Saturation of the SOS dependences at concentrations < $K_{HCII(SOS)}$ indicated that both $HCII_{free}$ and HCII·SOS react equally well with T·SOS, justifying the use of $[HCII]_o$ in Equation 5 (see "Experimental Procedures"). This analysis is based on the assumption of linkage of the equilibria in formation of ternary and higher order complexes shown in Scheme 1 (1). A hyperbolic analysis of k_{obs} depending solely on the HCII·SOS complex (44) produced fits incompatible with the data; HCII dependences at varying SOS were not resolved (Fig. 3*C*), and SOS dependences were only fit by $K_{HCII(SOS)}$ = 170 ± 40 μM, ~9-fold tighter than the experimentally observed value, demonstrating a requirement for thermodynamic equilibrium linkage and a contribution of T·SOS in ternary complex formation.

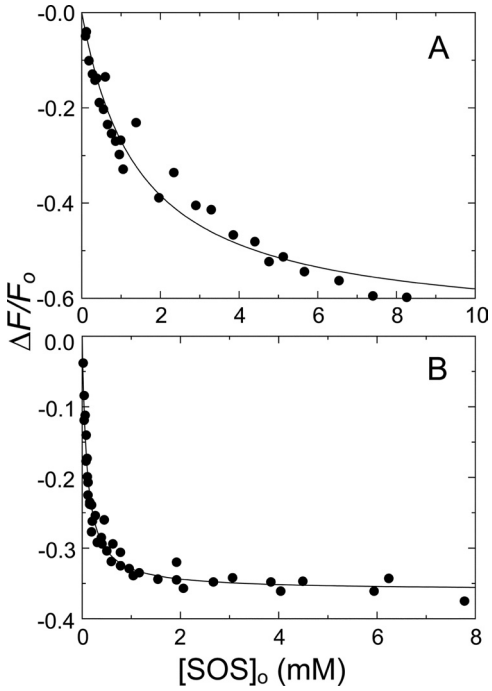

FIGURE 1. **Fluorescence equilibrium binding of SOS to HCII and AT bound to TNS.** *A*, fractional change in fluorescence ($\Delta F/F_o$) of 500 nM HCII and 12 μM TNS as a function of total SOS concentration ($[SOS]_o$). *B*, fractional change in fluorescence ($\Delta F/F_o$) of 3.7 and 4.5 μM AT and 12 μM TNS as a function of total SOS concentration. *Solid lines*, least squares fitting of the data by the quadratic equation for binding of a single ligand, with parameters $K_{HCII(SOS)}$ and $K_{AT(SOS)}$ given under "Experimental Procedures," $\Delta F_{max,HCII(SOS)}/F_o = -67 \pm 5\%$, and $\Delta F_{max,AT(SOS)}/F_o = -36 \pm 1\%$. Binding experiments were analyzed as described under "Experimental Procedures."

The SOS dependence of the apparent second-order rate constant k' is shown in Fig. 4*B*. Analysis of k' by Equation 6 with an offset of 0.0006 $\mu M^{-1}\ s^{-1}$ for the reaction in the absence of SOS gave 0.7 ± 0.1 $\mu M^{-1}\ s^{-1}$ for k'_{lim}, the maximal value of k' at saturating SOS, and K_{app} = 200 ± 60 μM, reflecting overall SOS

TABLE 1

Equilibrium binding and kinetic parameters for SOS-accelerated enzyme inactivation by HCII

Dissociation constants (K_D) for SOS binding to thrombin, Mz(-F1) and HCII were determined by equilibrium binding. Dissociation constants for overall binding of SOS to thrombin ($K_{T(SOS)app}$) and for ternary and higher order complex formation ($K_{complex}$), and limiting rates (k_{lim}) for thrombin inactivation were determined by kinetic analysis of the HCII and SOS concentration dependences by Equation 5. Second-order rate constants for thrombin, Mz(-F1), and MzT inactivation at SOS saturation were determined by Equation 6. Experiments were performed and analyzed as described under "Experimental Procedures." Errors represent ± 2 S.D.

	Equilibrium binding			Kinetics			
	Interaction	K_D	$\Delta F_{max}/F_o$	Interaction	K_D	k_{lim}	k'
		μM	%		μM	s^{-1}	$\mu M^{-1}\ s^{-1}$
SOS binding to T	$K_{T(SOS)}$ [a]	26 ± 5	−15 ± 1	$K_{T(SOS)app}$ [b]	200 ± 100		
	$K_{T(SOS)}$ [c]	17 ± 4	−13 ± 1	$K_{T(SOS)app}$ [d]	300 ± 100		
	$K_{T(SOS)}$ [e]	10 ± 4	−10 ± 2				
SOS binding to Mz(-F1)	$K_{T(SOS)_2}$ [e]	400 ± 300	−8 ± 2				
	$K_{Mz(-F1)(SOS)}$ [a]	1600 ± 500	−15 ± 1				
SOS binding to HCII	$K_{HCII(SOS)}$ [a]	1450 ± 300	−67 ± 5				
Complex affinity, limiting rate, second-order rate constant				$K_{complex}$ [b]	0.12 ± 0.04	0.12 ± 0.02	1.0 ± 0.1
				$K_{complex}$ [d]	0.20 ± 0.10	0.15 ± 0.05	0.8 ± 0.1
				$K_{complex,Mz(-F1)}$ [b]			0.9 ± 0.1
				$K_{complex,MzT}$ [f]			0.4 ± 0.1

[a] Single ligand.
[b] Global fit.
[c] Single ligand and slope.
[d] HCII dependence.
[e] Two sites.
[f] SOS dependence.

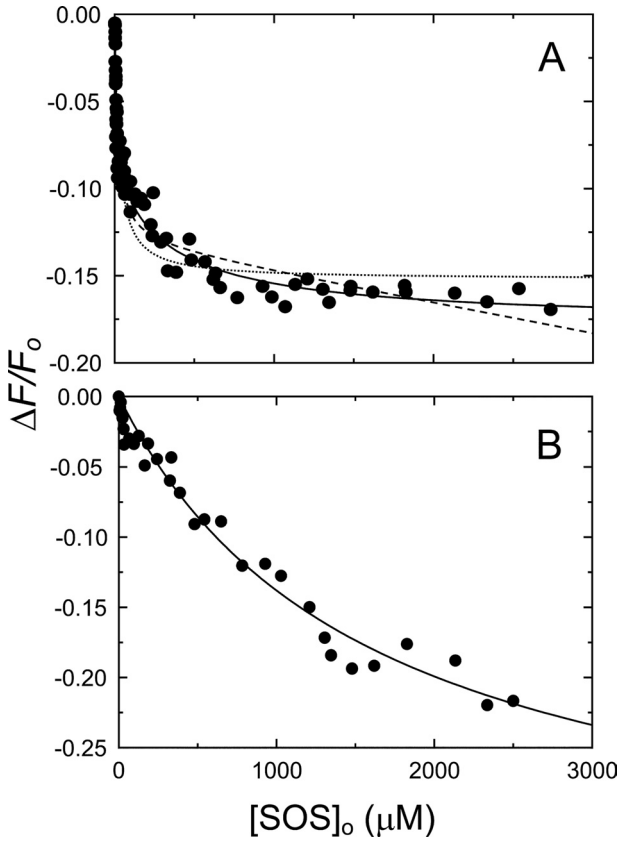

FIGURE 2. **Fluorescence equilibrium binding of SOS to [ANS]FPR-T and [ANS]FPR-Mz(-F1).** *A*, fractional change in fluorescence ($\Delta F/F_o$) of 390 nM [ANS]FPR-T as a function of total SOS concentration ($[SOS]_o$). *Solid lines*, least squares fits of the data by Equation 1, with the parameters $K_{T(SOS)}$ and $K_{T(SOS)_2}$ listed under "Results." *Dashed lines*, fitting by the quadratic equation for binding of a single ligand, with or without a nonspecific term. *B*, fractional change in fluorescence ($\Delta F/F_o$) of 343 nM [ANS]FPR-Mz(-F1) as a function of total SOS concentration. *Solid lines*, least squares fits of the data by the quadratic equation for binding of a single ligand. Binding experiments were analyzed as described under "Experimental Procedures."

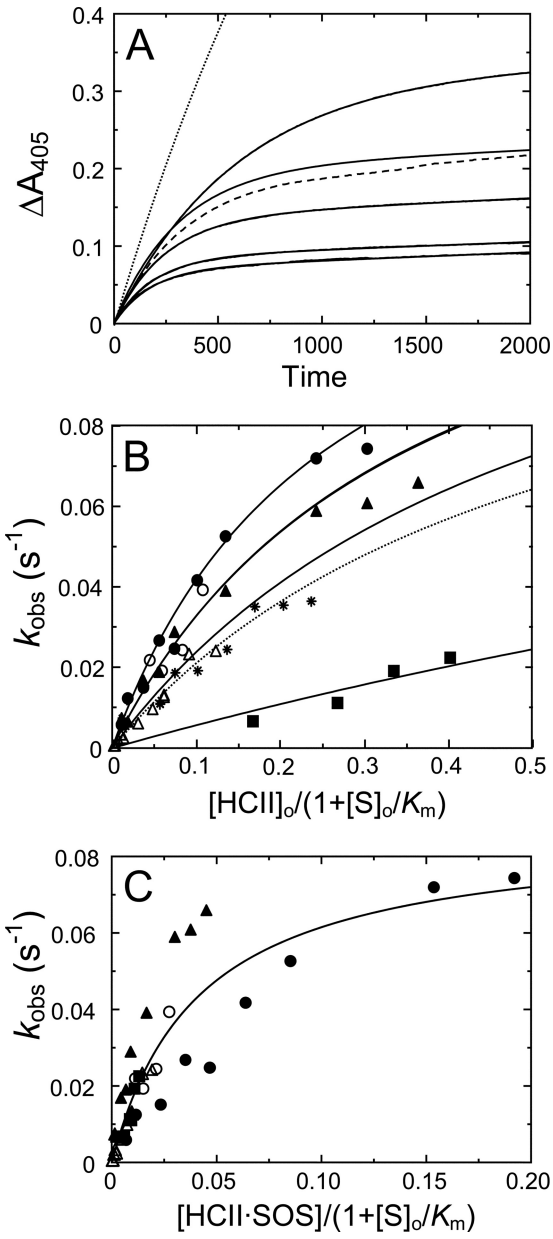

FIGURE 3. **HCII concentration dependences of the inactivation kinetics.** *A*, an array of progress curves for inactivation of 0.5 nM thrombin (*solid lines*) by 166 nM HCII, in the presence of Chromozym TH (156 μM) and increasing concentrations of SOS (in order of decreasing amplitude: 170, 345, 430, 600 and 2000 μM). *Dashed line*, a reaction of 4 nM stable MzT with 166 nM HCII, at 156 μM Chromozym TH and 2000 μM SOS. *Dotted line*, a thrombin control reaction with 166 nM HCII, at 156 μM Chromozym TH and 20 mM Na_2SO_4. *B*, first-order inactivation rate constants (k_{obs}) as a function of effective total HCII concentration ($[HCII]_o/(1 + [S]_o/K_m)$), at 2500 μM (●), 207 μM (▲), and 50 μM SOS (■) and 156 μM Chromozym TH; 500 μM SOS (○) and 198 μM Chromozym TH; or 500 μM SOS (△) and 200 μM S2238. *Solid lines* represent global least squares fitting of the combined data by Equation 5, with the parameters listed under "Results." Data for Mz(-F1) inactivation at 518 μM SOS and 156 μM Chromozym TH are indicated by *asterisks*. *C*, first-order inactivation rate constants (k_{obs}) for the same data sets in *B*, as a function of effective HCII·SOS concentration ($[HCII \cdot SOS]/(1 + [S]_o/K_m)$), without equilibrium linkage and SOS binding to thrombin. Experiments were analyzed as described under "Experimental Procedures."

binding in the complex. Good agreement was observed between reactions with Chromozym TH and CBS31.39.

Individual contributions of the pathways in Scheme 1 toward higher order complexes, calculated by numerical integration, are shown in Fig. 5*A*–*C*. Rate and equilibrium constants were fixed at the determined values, and $K_{HCII \cdot SOS(T)}$ was calculated from detailed balance. Fig. 5*A* shows a time scale, including disappearance of free thrombin and formation of the covalent T-HCII complex. The pathway contributions as a function of HCII (Fig. 5*B*) and SOS (Fig. 5*C*) illustrate the predominance of the T·SOS-HCII and T·SOS-HCII·SOS pathways. The sum of all of the pathway contributions *versus* HCII and SOS concentration mirrors the HCII and SOS dependences of the experimentally obtained inactivation rates, k_{obs}.

Specificity of SOS for the Thrombin-HCII Interaction—Although SOS bound to AT, it did not accelerate thrombin inactivation by AT but had a modest inhibitory effect on the reaction, as shown in Fig. 6*A*. The second-order rate constant k' in the absence of SOS was 7600 ± 800 M^{-1} s^{-1} and decreased to 6700 ± 400 and 4600 ± 600 M^{-1} s^{-1} in the presence of 50 and 500 μM SOS, respectively. The effect of SOS binding to AT on the inactivation of fXa accelerated by the synthetic pentasaccharide fondaparinux is shown in Fig. 6*B*. Fondaparinux binds to the heparin-binding site on AT, with K_D = 50–60 nM (54). The apparent second-order rate constant for fXa reacting with AT at 500 nM fondaparinux was 0.55 ± 0.01 μM^{-1} s^{-1} (*trace a*),

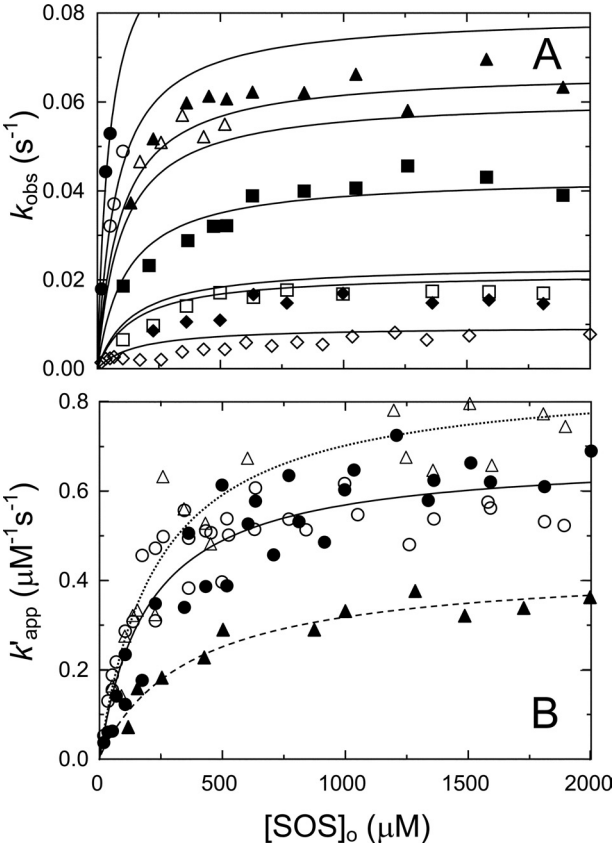

FIGURE 4. **SOS concentration dependences of the inactivation kinetics.** *A*, first-order inactivation rate constants (k_{obs}) as a function of total SOS ([SOS]$_o$) concentration, at various fixed HCII and chromogenic substrate concentrations: 553 nM (●), 277 nM (○), 197 nM (▲), 166 nM (△), 98 nM (■), 45 nM HCII (□), and 150 μM CBS31.39; 415 nM (◆) and 166 nM HCII (◇); and 157 μM Chromozym TH. *Solid lines*, global least squares fitting of the combined data by Equation 5, with the parameters $K_{T(SOS)app}$, $K_{complex}$, k_{lim}, and $K_{HCII(SOS)}$ given under "Results." *B*, the apparent second-order rate constant (k') for thrombin inactivation by HCII as a function of total SOS concentration, obtained from reactions in the presence of Chromozym TH (●) and CBS31.39 (○), and for Mz(-F1) (△) and MzT (▲) inactivation in the presence of Chromozym TH or CBS31.39. *Solid* (T), *dotted* (Mz(-F1)), and *dashed lines* (MzT), least squares fitting of the data by Equation 6, with parameters given under "Results." Experiments were analyzed as described under "Experimental Procedures."

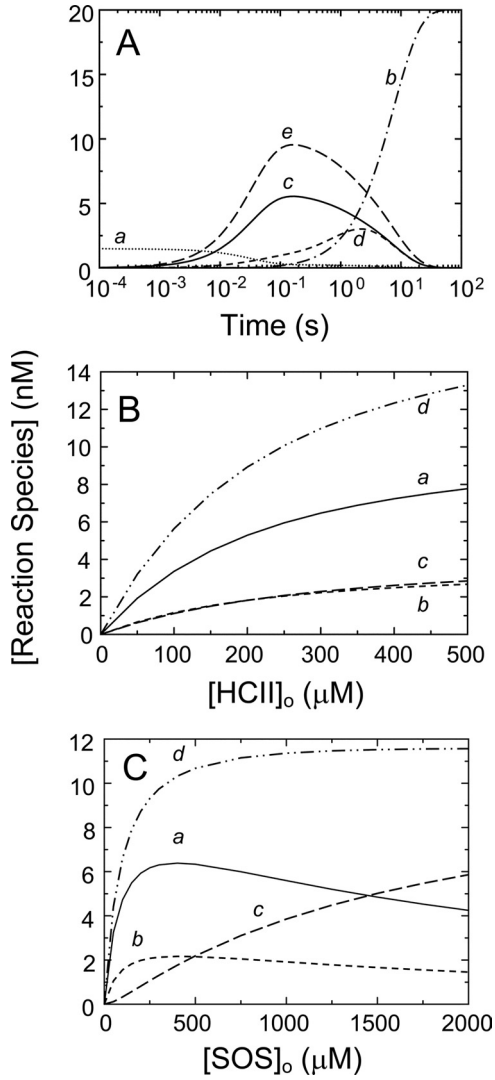

FIGURE 5. **Individual contributions of SOS-bound species to higher order complex formation, based on numerical integration.** *A*, time scale showing disappearance of free thrombin (*trace a*) and generation of covalent complex (*trace b*) in addition to generation of intermediate complex from T·SOS and HCII (*trace c*), from HCII·SOS and T (*trace d*), and from T·SOS and HCII·SOS (*trace e*). SOS, thrombin, and HCII concentrations were 2500 μM, 20 nM, and 1 μM, respectively. *B*, HCII dependences of the higher order complexes of SOS, thrombin, and HCII ([*Reaction species*]) formed from T·SOS and HCII (*trace a*), from HCII·SOS and T (*trace b*), and from T·SOS and HCII·SOS (*trace c*) and the sum of the three pathways (*trace d*). Thrombin and SOS concentrations were 27 nM and 500 μM, respectively. *C*, SOS dependences of the higher order complexes of SOS, thrombin, and HCII formed from T·SOS and HCII (*trace a*), from HCII·SOS and T (*trace b*), and from T·SOS and HCII·SOS (*trace c*) and the sum of the three pathways (*trace d*). Thrombin and HCII concentrations were 27 and 166 nM, respectively. All forward rate constants were 32 $\mu M^{-1} s^{-1}$; $K_{T(SOS)app}$ was 200 μM; $K_{complex}$ was 0.12 μM, representing both k_{-2}/k_{+2} and k_{-5}/k_{+5}; $K_{HCII(SOS)}$ was 1.45 mM; $K_{HCII\cdot SOS(T)}$ was 0.028 μM, as a result of the equilibrium linkage. The chemical step, $k_{lim} = 0.12\ s^{-1}$, determined covalent T-HCII complex formation.

in good agreement with previously reported values (43, 55), and decreased to 0.46 ± 0.01 and 0.14 ± 0.01 $\mu M^{-1} s^{-1}$ in the presence of 200 and 2000 μM SOS, respectively (*traces b* and *c*), indicating that the pentasaccharide and SOS share partially overlapping binding sites on AT. In control reactions without fondaparinux, SOS at 2000 μM had only a marginally accelerating effect on the inactivation of fXa by AT (*trace d*).

Role of Exosite I in the SOS-accelerated T-HCII Reaction—Titrations of [5F]Hir-(54–65)(SO_3^-) with thrombin in the absence and presence of SOS gave $K_{T(Hir)}$ = 22 ± 3 nM and $\Delta F_{max,T(Hir)}/F_o = -32 \pm 1\%$ (Fig. 7*A*), in good agreement with reported values (33). SOS binding to thrombin did not affect binding of the peptide to exosite I. The effect of Hir-(54–65)(SO_3^-) on the SOS-accelerated T-HCII reaction is shown in Fig. 7*B*. Simultaneous analysis of the data by Equation 7 and the binding equation for Hir-(54–65)(SO_3^-) binding to thrombin gave second-order rate constants k'_i = 0.63 ± 0.03 $\mu M^{-1} s^{-1}$ and $k'_{T\cdot SOS(Hir)}$ = 0.10 ± 0.10 $\mu M^{-1} s^{-1}$, reflecting the contributions of T·SOS and the T·SOS·Hir-(54–65)(SO_3^-) complex reacting with HCII, respectively. At 518 μM SOS, thrombin (27 nM) was predominantly present as T·SOS complex. The dissociation constant $K_{T\cdot SOS(Hir)}$ for binding of Hir-(54–65)(SO_3^-) to T·SOS during inactivation was 30 ± 20 μM, much higher than the independently determined equilibrium binding value of 22 nM. This result was consistent with binding of Hir-(54–65)(SO_3^-) to a subsite on exosite I that only partially overlaps with the binding site for the HCII NH_2-terminal segment.

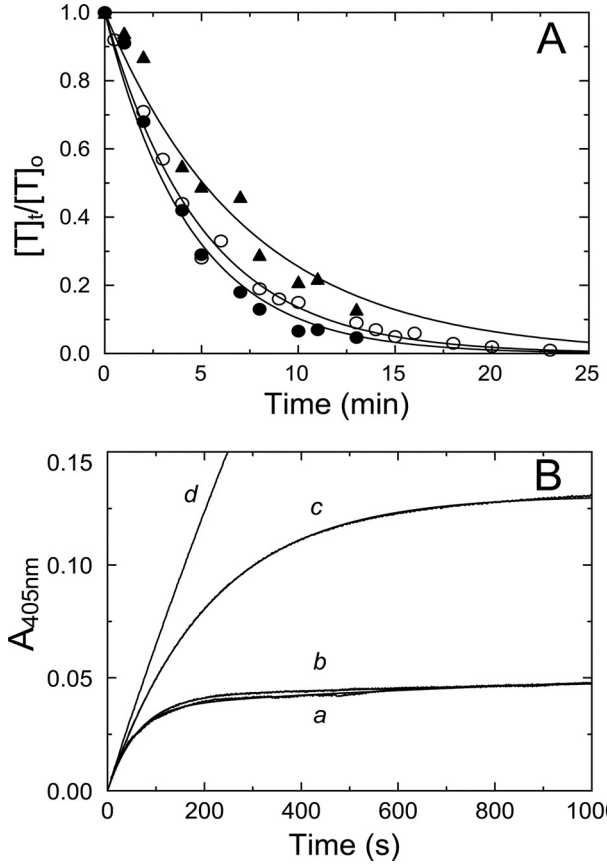

FIGURE 6. **Selectivity of SOS for thrombin inactivation by HCII.** *A*, fractional thrombin activity ($[T]_f/[T]_o$) as a function of time is shown for reactions of 500 nM AT and 50 nM T, in the absence (●), and the presence of 50 μM (○), and 500 μM (▲) SOS. *Solid lines*, fit of the data by a single exponential. Values for *k′* for each reaction are given under "Results." *B*, progress curves for inactivation of 0.6 nM fXa by 65 nM AT in the presence of Spectrozyme fXa (160 μM) and fondaparinux (500 nM). Reactions were performed in the absence (*a*) and the presence of 200 μM (*b*) and 2000 μM (*c*) SOS. The control reaction (*d*) had 2000 μM SOS and no fondaparinux. *Solid lines*, nonlinear least squares fits of the data by Equations 2–4. Inactivation reactions were analyzed as described under "Experimental Procedures."

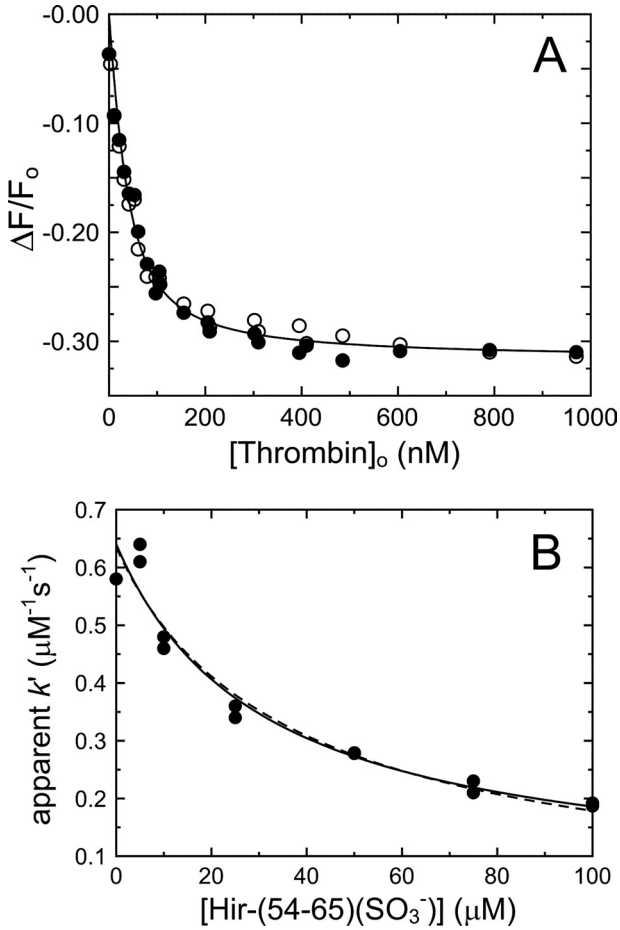

FIGURE 7. **Effect of Hir-(54–65)(SO_3^-) on thrombin inactivation by HCII.** *A*, fractional change in fluorescence ($\Delta F/F_o$) of 29 nM [5F]Hir-(54–65)(SO_3^-) as a function of total thrombin concentration ($[Thrombin]_o$). *Solid lines*, least squares fits by the quadratic equation for binding of a single ligand, with $\Delta F_{max,T(Hir)}/F_o$ and $K_{T(Hir)}$ given under "Results" for titrations in the absence (●) and presence (○) of 518 μM SOS. *B*, dependence of the apparent bimolecular rate constant (*k′*) on the total concentration of Hir-(54–65)(SO_3^-). *Solid line*, least squares fit of the data by Equation 7 combined with the quadratic binding equation for Hir-(54–65)(SO_3^-) binding to T·SOS, with the fitted parameters *k′* and $k^-_{T\cdot SOS(Hir)}$ listed under "Results." *Dashed line*, fit by the purely competitive model for binding of peptide and HCII to exosite I. Experiments were analyzed as described under "Experimental Procedures."

The fit by a model for purely competitive binding of Hir-(54–65)(SO_3^-) and HCII to T·SOS (Fig. 6*B*, *dashed line*) was indistinguishable from that by Equation 7 (*solid line*). However, the fitted $K_{T\cdot SOS(HCII)}$ of 90 ± 20 pM represented a 1300-fold tighter interaction of the HCII NH_2-terminal segment with T·SOS, inconsistent with $K_{complex}$ of 0.12–0.20 μM from the inactivation kinetics. If such a tight interaction between HCII and thrombin were to occur, complete saturation of the HCII dependence of k_{obs} would have been observed at even the lowest experimental HCII concentrations. On this basis, the model allowing partially overlapping subsites was chosen over that for mutually exclusive binding.

Role of Exosite II in the SOS-accelerated T-HCII Reaction—Inactivation of MzT and Mz(-F1) was measured at varying SOS and HCII, and the effect of exosite II aptamer HD-22 on thrombin inactivation was explored. The Mz(-F1) data were fit globally by Equation 5, using $K_{Mz(-F1)(SOS)}$ of 1600 μM from equilibrium binding, and were consistent with a second-order rate constant $k_{lim}/K_{complex}$ of 0.9 ± 0.1 $\mu M^{-1}\ s^{-1}$, demonstrating that Mz(-F1) and thrombin were inactivated at comparable rates (Figs. 3*B* and 4*B*). MzT inactivation was ~50% slower (Fig. 3*A*, *dashed line*, and Fig. 4*B*) and was characterized by a limiting apparent rate constant of 0.4 ± 0.1 $\mu M^{-1}\ s^{-1}$. Thrombin inactivation reactions at 500 nM HCII, 500 μM SOS, and 120 μM Chromozym TH in the absence and presence of 1.2 μM thrombin exosite II aptamer HD-22 had comparable apparent *k′* values of 0.44 and 0.39 ± 0.01 $\mu M^{-1}\ s^{-1}$ (data not shown). These results suggest that thrombin exosite II is not significantly involved in SOS-accelerated inactivation by HCII.

Thrombin Generation in Normal (PNP) and HCII-immunodepleted Plasma—Thrombin generation in PNP was measured by CAT in the absence and presence of SOS. fXa (3 nM) and TF (16 pM) triggered robust thrombin generation (Fig. 8, *A* and *B*, *trace a*), attenuated by increasing SOS concentrations (*traces b–f*). The decrease in ETP (Fig. 8, *A* and *B*, *inset*) as a function of SOS was hyperbolic, with SOS at half-maximal ETP values of 160 ± 20 μM (fXa trigger) and 200 ± 30 μM (TF trigger) (Equation 8). The $CaCl_2$ assay concentration (17 mM)

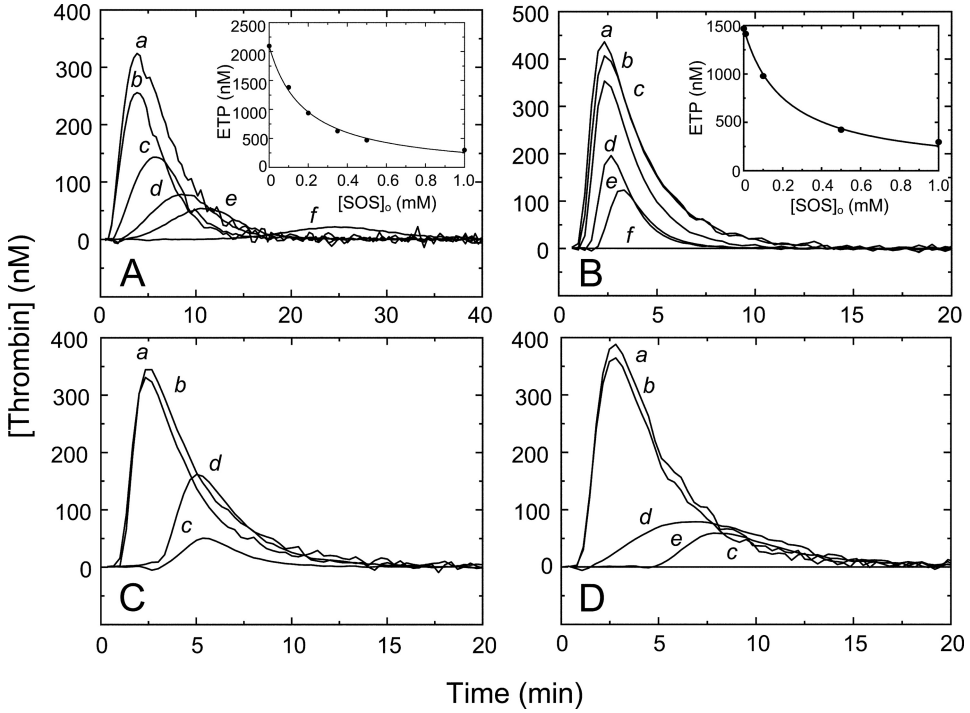

FIGURE 8. **SOS-mediated inhibition of thrombin generation and effect of anti-HCII antibodies.** *A*, thrombin generation ([Thrombin]) in PNP, triggered by 3 nM fXa, in the presence of 0, 100, 200, 350, 500, and 1000 μM SOS (*traces a–f*). *Inset*, endogenous thrombin potential (*ETP*) as a function of total SOS concentration in the plasma ([SOS]$_o$). The *solid line* represents the least squares fit of the data by Equation 8, with the fitted parameters ETP$_o$ = 2100 ± 100 nM and *A* = 160 ± 20 μM. *B*, thrombin generation triggered by 16 pM TF, in the presence of 0, 10, 100, 500, 1000, and 5000 μM SOS (*traces a–f*). *Inset*, ETP as a function of total SOS concentration in the plasma ([SOS]$_o$). Fitted parameters were ETP$_o$ = 1470 ± 40 nM and *A* = 200 ± 30 μM. *C*, thrombin generation triggered by 16 pM TF, at 0 μM SOS, in the absence (*trace a*) and the presence (*trace b*) of 6 μM goat anti-human HCII antibody, and at 2000 μM SOS, in the absence (*trace c*) and presence (*trace d*) of antibody. *D*, thrombin generation triggered by 16 pM TF, at 0 μM SOS, in the absence (*trace a*) and the presence (*trace b*) of 6 μM sheep anti-human HCII antibody, and at 1000 and 5000 μM SOS, in the absence (*trace c*) and presence (*traces d* and *e*) of antibody. CAT assays were analyzed as described under "Experimental Procedures."

compensated adequately for possible Ca^{2+}-chelating effects of SOS (22).

The effects of polyclonal sheep and goat anti-human HCII antibodies in TF-triggered assays are shown in Fig. 8, *C* and *D*. The goat antibody (6 μM) restored 53% of the original ETP in TF-triggered assays at 2000 μM SOS (Fig. 8*C*). The sheep antibody (6 μM) restored 30 and 22% of the ETP in TF- and fXa-triggered assays at 1 and 5 mM SOS, respectively (Fig. 8*D*).

The effects of SOS and heparin-depleted DS on fXa- and TF-triggered thrombin generation in HCII-depleted plasma are shown in Fig. 9, *A* and *B*. Both SOS and DS caused an HCII-independent decrease of thrombin generation. The decrease in ETP as a function of SOS concentration (Fig. 9*B*, *inset*) was significant but much less pronounced than that observed with PNP, with a 3-fold increase of the SOS concentration to 600 ± 100 μM at half-maximal ETP. Suppression of thrombin generation (Fig. 9*C*) and decrease in ETP (Fig. 9*C*, *inset*) were observed in HCII-depleted plasma supplemented with 0.7–3.9 μM purified HCII. The observed differences in ETP$_o$ and peak height for PNP- and HCII-depleted plasmas were due to batch-to-batch variability. In separate *in vitro* experiments, SOS delayed prothrombin activation by the prothrombinase complex in the presence of 80:20 phosphatidylcholine/phosphatidylserine phospholipids (Fig. 9*D*), which may explain the HCII-independent contribution of SOS to suppression of thrombin generation.

DISCUSSION

These studies describe the previously unreported observation that, *in vitro*, the sulfated disaccharide SOS enhances thrombin inactivation by HCII up to 2000-fold. The data are consistent with a mechanism by which inactivation is accelerated through allosteric engagement of the HCII NH_2-terminal segment with exosite I on SOS-bound thrombin. According to Scheme 1 and the experimental parameters, higher order complexes preceding covalent inactivation are formed by T·SOS reacting with HCII·SOS, at SOS concentrations around and exceeding the dissociation constant for SOS binding to HCII, with a significant contribution of T·SOS reacting with free HCII at SOS concentrations below this value. The data are not compatible with a model in which inactivation is exclusively driven by HCII·SOS formation and SOS binding to thrombin does not play a role (44). With this model, HCII·SOS dependences of k_{obs} are overlapping due to the assumption that saturation of T with SOS does not affect the inactivation rate. Our data were fit very well by a model that does contain the linkage factor $(1 + K_{T(SOS)app}/[SOS]_{free})$ implicating a role for T·SOS and uses $[HCII]_o$, the sum of [HCII·SOS] and $[HCII]_{free}$, as the independent variable (Equation 5). Similarly, the SOS dependences could not be fit adequately by the non-linkage model. Our findings suggest a mechanism of linked equilibria in the formation of ternary and quaternary complexes, involving T·SOS in the inactivation reactions (1).

Thrombin saturates at SOS concentrations below those required for saturation of HCII, favoring the presence of T·SOS complexes reacting both with free and SOS-complexed HCII. Individual kinetic contributions of the two thrombin sites were not resolvable, as demonstrated by single hyperbolic behavior of the SOS dependences. Consequently, overall SOS binding to thrombin, reflecting combined contributions from both species, was described by the apparent dissociation constant $K_{T(SOS)app}$. Partial saturation of k_{obs} was observed at 2.5 mM SOS, with 60% of HCII present as HCII·SOS, indicative of a mechanism in which both $HCII_{free}$ and HCII·SOS assemble with comparable affinity into reversible T·SOS·HCII and T·SOS·HCII·SOS complexes that react to form covalent T-HCII species. The $K_{complex}$ value of 0.12–0.20 μM for binding of T·SOS to $HCII_{free}$ and HCII·SOS indicated a ~10,000-fold

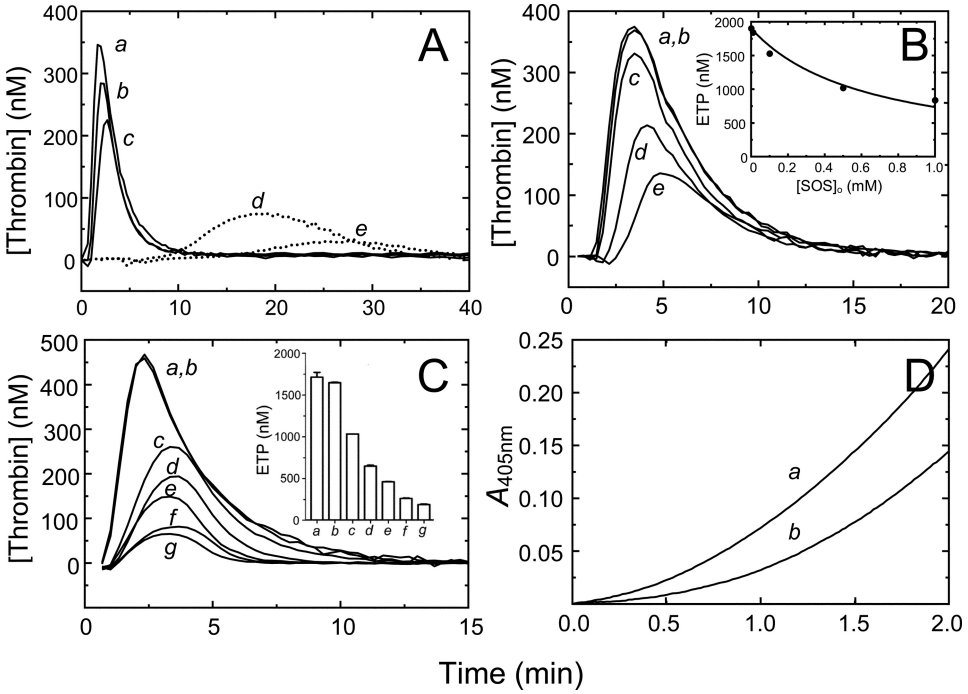

FIGURE 9. **Effect of SOS on thrombin generation in HCII-depleted plasma and in a purified system.** *A*, thrombin generation ([Thrombin]) in HCII-depleted plasma, triggered by 3 nM fXa, at 0, 250, and 500 μM SOS (*traces a–c*), and at 0.5 and 1 μM heparin-free DS (*traces d and e*, *dotted lines*). *B*, thrombin generation triggered by 16 pM TF, at 0, 10, 100, 500, and 1000 μM SOS (*traces a–e*). *Inset*, ETP as a function of total SOS concentration in the plasma ([SOS]$_o$). *C*, thrombin generation triggered by 3 nM fXa, in the absence of SOS, and in the absence (*trace a*) and presence (*trace b*) of 1.3 μM supplemented purified plasma HCII. *Traces c–g* are in the presence of 250 μM SOS, at 0, 0.67, 1.3, 2.6, and 3.9 μM HCII, respectively. *Inset*, ETP for reactions *a–g*. CAT assays were analyzed as described under "Experimental Procedures." *D*, *in vitro* prothrombin activation, in the absence (*trace a*) and presence of 600 μM SOS, as described under "Experimental Procedures."

tightening of HCII binding to thrombin exosite I and SOS in these complexes. Numerical integration analysis of the mechanism (Scheme 1) showed predominantly T·SOS binding to $HCII_{free}$ and HCII·SOS before rate-limiting covalent complex formation.

Template-forming GAGs assist the allosteric interaction by approximation of thrombin and HCII on a single GAG chain, with tightening of HCII binding in the ternary complex to $K_{complex}$ values of 0.5–5 nM (9, 56). The respective GAG affinities for thrombin and HCII or AT determine their partitioning in binary complexes, and the linkage of the dissociation constants for the binary and ternary complexes dictates the preferred pathways of ternary complex formation (1, 57, 58). As a result, AT·heparin is the predominant intermediate in T-AT reactions with high affinity heparin, whereas T·heparin is prevalent in T-AT reactions with low affinity heparin (1, 58) and T-HCII reactions with heparin and DS (9, 56). In the latter, allosteric engagement is triggered by HCII binding to GAG of the T·GAG complex (9, 56). Saturation of both thrombin and serpin with template GAGs results in a quaternary complex with reduced reactivity due to steric hindrance, and for the T-AT reaction, the separate contributions of the ternary and quaternary complex components have been quantitated (1). With SOS, these contributions did not resolve into two components, suggesting equally reactive T·SOS·HCII and T·SOS·HCII·SOS complexes with comparable k_{lim} and $K_{complex}$ and consistent with the absence of significant steric hindrance associated with T·SOS binding to HCII·SOS. The selectivity of SOS for accelerating thrombin inactivation by HCII, but not AT, is attributed to its potential for triggering the allosteric interaction, absent in the T-AT reaction.

A sulfated DS hexasaccharide with high affinity for HCII (20) and bis-lactobionic and bis-maltobionic acid amides, all non-template compounds, selectively accelerate inhibition by HCII (18, 20, 59–63), and their action was attributed exclusively to triggering of the allosteric reaction. Whether these compounds bind thrombin is unknown, and they may catalyze thrombin inactivation by a mechanism that exclusively employs binding to HCII. In this respect, their mode of action may be different from that of SOS.

Allosteric interaction of HCII with thrombin requires tightened HCII binding in the higher order complexes with SOS, as evidenced by $K_{complex}$ = 0.12–0.20 μM. This combines all forces that hold the complex together, including the tightened interaction of HCII with SOS upon binding of thrombin, the interactions between the HCII reactive center loop and the thrombin active site, the interactions between the HCII NH_2-terminal segment and thrombin exosite I, and the unusually extensive intermolecular contacts at the interface between thrombin and HCII (16). Whereas chromogenic substrates make contact solely with the S1–S3 specificity pocket of the enzyme, extended contacts exist between the active site and the HCII reactive center loop, involving P4–P5′ residues (16), possibly explaining the lack of pronounced effects of SOS binding to thrombin on chromogenic substrate hydrolysis. The NH_2-terminally truncated Δ74 HCII, mimicking HCII with an altered conformation in the heparin-binding site, binds tighter to heparin-Sepharose than plasma HCII (3), suggesting that this altered conformation binds tighter to heparin in the ternary complex with thrombin, although the lack of *N*-glycosylation in the heparin binding site may be partially responsible for tighter binding (64).

The similar rates of inactivation of thrombin in the absence and presence of saturating, tightly binding exosite II aptamer (50) and the comparable rates of thrombin and Mz(-F1) inactivation suggest that an accessible exosite II is not obligatory for effective inactivation. Thrombin, MzT, and Mz(-F1) are Na^+-activated enzymes existing in three conformations with different reactivity (42, 65). Thrombin and Mz(-F1) exhibit similar Na^+ binding characteristics, whereas Na^+ binding to MzT is significantly weaker (42, 65). The ~50% reduced inactivation rates observed for MzT may reflect this difference in Na^+ activation and may suggest the requirement of a fully Na^+-activated species for optimal reaction with HCII.

SOS is a structurally flexible heparin mimetic (66), binding to fibroblast growth factors (67–69), bridging fibroblast growth factors and their receptors (70, 71), and binding to follistatin (72). The sulfate groups can form hydrogen bonds with Lys, Arg, Gly, Asp, Asn, Ser, Met, Gln, and Ala. The structural flexibility of SOS and its charge distribution properties may explain its unusual capability of bridging large molecules. It is unknown whether such a bridging exists between thrombin and HCII at the interface in the Michaelis complex. A heparin/DS binding site has been demonstrated on Mz(-F1) (9) and may also bind SOS. Whether SOS bound to this site can make contact with any part of HCII, possibly triggering allosteric conformational change, remains to be resolved.

As shown here, SOS binds AT at the heparin-binding site, and the binding sites of SOS and fondaparinux overlap. Fractional occupation of AT by fondaparinux (500 nM) and SOS (2000 μM) was 29 and 68%, respectively, with ~3% free AT remaining. The apparent rate constant for the fondaparinux-catalyzed fXa inactivation by AT decreased to 25% of its original value in the absence of SOS, in good agreement with the fractional occupation of 29%, indicating that the binding sites for SOS and fondaparinux on AT are mutually exclusive. These results may suggest that, similarly, SOS binds to the corresponding heparin-binding site on HCII. The binding subsites for heparin and DS on HCII are partially overlapping (73), and SOS may bind to either subsite. However, the GAG-binding site on HCII may not be the only binding site for SOS. Although the data for SOS binding to HCII was analyzed adequately with a 1:1 stoichiometry, multiple binding sites on HCII cannot be excluded, because stoichiometric titrations with HCII $\cong K_{HCII(SOS)}$ were experimentally unattainable. The studies do not exclude the possibility of SOS binding interactions on HCII, not reported by TNS, elsewhere than the heparin-binding site of HCII. However, non-heparin-binding site interactions, tighter than those observed with thrombin and instrumental in ternary or higher complex formation by a pathway governed by HCII·SOS complex, would still result in k_{obs} dependences of HCII that are unresolved at varying degrees of thrombin binding to SOS and would show more pronounced saturation than is experimentally observed. This further supports a mechanism utilizing the T·SOS complex in a pathway toward ternary or quaternary complex formation.

The attenuating effect of Hir-(54–65)(SO_3^-) on thrombin inactivation was consistent with a model in which the peptide and HCII share overlapping binding sites on exosite I (16, 74), resulting in a weaker apparent binding of the peptide to thrombin. A purely competitive model required an extremely tight interaction of HCII with exosite I, in disagreement with $K_{complex}$ of ~0.12–0.20 μM. In the uncatalyzed thrombin-AT reaction, Hir-(54–65)(SO_3^-) displacement is competitive and parallels exosite I crushing during inactivation, with a peptide dissociation constant of 16 nM similar to $K_{T(Hir)}$ 26 nM from equilibrium binding (33). Binding of HCII to exosite I, absent in AT, may result in a conformational intermediate preceding exosite I crushing.

The physiological potential of SOS was demonstrated by thrombin generation in human plasma *ex vivo*. A previous study indicated that 650 μM SOS did not significantly prolong the prothrombin and thrombin times in clotting assays but had an effect similar to that of a 50-fold lower heparin concentration on the partial thromboplastin time, which was attributed to chelating effects of SOS (22). However, clot formation is an end point in these assays, and the clot is already formed when only ~5% of thrombin generation has occurred (75). Thrombin generation was measured at 17 mM $CaCl_2$ to neutralize the citrate in plasma and SOS chelation. Substantial but not complete restoration of thrombin generation by anti-HCII polyclonal antibodies was observed, mainly due to SOS attenuating prothrombin activation. Bis-lactobionic and bis-maltobionic acid amides were also reported to delay prothrombin activation (62). Thrombin generation in HCII-depleted plasma was suppressed both by SOS and HCII-specific DS. This suggests an additional anticoagulant mechanism for SOS and DS, different from the bis-lactobionic acid amide that reportedly did not cause a decrease in thrombin generation in HCII-depleted plasma (63). The SOS concentration at half-maximal ETP in PNP was 3-fold lower than that in HCII-depleted plasma, and significant exogenous HCII-dependent decrease of the ETP was observed in HCII-depleted plasma, strongly suggesting a role for SOS in HCII-mediated thrombin inactivation *in vivo*.

In anticoagulation therapy, heparin-catalyzed thrombin and fXa inactivation by AT are central in management of venous thrombosis and disseminated intravascular coagulation (76), whereas regulation of thrombin activity by HCII has been identified as a key process in inhibition of arterial thrombosis (77), disseminated intravascular coagulation associated with inflammatory diseases (78), and certain cancers (79). Selective inactivation of thrombin on localized, DS-rich surfaces by HCII rather than AT may be an important part of physiological regulation of thrombin activity *in vivo*. In addition, oral administration of the gastroprotective aluminum SOS (sucralfate) in a rodent model was demonstrated to result in gastrointestinal absorption of the SOS sodium salt and significant redistribution of SOS to the aortic endothelium (80), suggesting a potential for bioavailability specifically targeted toward areas where anticoagulation is critical. The present study supports an anticoagulant mechanism in which low M_r, highly sulfated oligosaccharides, such as SOS, target the thrombin-HCII interaction through triggering of the allosteric HCII-thrombin engagement by SOS binding both to thrombin and HCII.

Acknowledgment—We thank Dr. P. E. Bock for helpful discussions and critique of the manuscript.

REFERENCES

1. Olson, S. T. (1988) *J. Biol. Chem.* **263,** 1698–1708
2. Tollefsen, D. M., Pestka, C. A., and Monafo, W. J. (1983) *J. Biol. Chem.* **258,** 6713–6716
3. Van Deerlin, V. M., and Tollefsen, D. M. (1991) *J. Biol. Chem.* **266,** 20223–20231
4. Rogers, S. J., Pratt, C. W., Whinna, H. C., and Church, F. C. (1992) *J. Biol. Chem.* **267,** 3613–3617
5. Church, F. C., Meade, J. B., Treanor, R. E., and Whinna, H. C. (1989) *J. Biol. Chem.* **264,** 3618–3623
6. Hayakawa, Y., Hayashi, T., Lee, J., Srisomporn, P., Maeda, M., Ozawa, T., and Sakuragawa, N. (2000) *Biochim. Biophys. Acta* **1543,** 86–94
7. Stubbs, M. T., and Bode, W. (1993) *Thromb. Res.* **69,** 1–58

8. Bode, W., Turk, D., and Karshikov, A. (1992) *Protein Sci.* **1,** 426–471
9. Verhamme, I. M., Bock, P. E., and Jackson, C. M. (2004) *J. Biol. Chem.* **279,** 9785–9795
10. Bauman, S. J., and Church, F. C. (1999) *J. Biol. Chem.* **274,** 34556–34565
11. Colwell, N. S., Grupe, M. J., and Tollefsen, D. M. (1999) *Biochim. Biophys. Acta* **1431,** 148–156
12. Danielsson, A., Raub, E., Lindahl, U., and Björk, I. (1986) *J. Biol. Chem.* **261,** 15467–15473
13. Hortin, G. L., Tollefsen, D. M., and Benutto, B. M. (1989) *J. Biol. Chem.* **264,** 13979–13982
14. Ragg, H., Ulshöfer, T., and Gerewitz, J. (1990) *J. Biol. Chem.* **265,** 22386–22391
15. Myles, T., Church, F. C., Whinna, H. C., Monard, D., and Stone, S. R. (1998) *J. Biol. Chem.* **273,** 31203–31208
16. Baglin, T. P., Carrell, R. W., Church, F. C., Esmon, C. T., and Huntington, J. A. (2002) *Proc. Natl. Acad. Sci. U.S.A.* **99,** 11079–11084
17. Mitchell, J. W., and Church, F. C. (2002) *J. Biol. Chem.* **277,** 19823–19830
18. Martin, D. J., Toce, J. A., Anevski, P. J., Tollefsen, D. M., and Abendschein, D. R. (1999) *J. Pharmacol. Exp. Ther.* **288,** 516–521
19. Klauser, R. J. (1991) *Thromb. Res.* **62,** 557–565
20. Maimone, M. M., and Tollefsen, D. M. (1990) *J. Biol. Chem.* **265,** 18263–18271
21. Nagashima, R. (1981) *J. Clin. Gastroenterol.* **3,** Suppl. 2, 117–127
22. Fannon, M., Forsten-Williams, K., Nugent, M. A., Gregory, K. J., Chu, C. L., Goerges-Wildt, A. L., Panigrahy, D., Kaipainen, A., Barnes, C., Lapp, C., and Shing, Y. (2008) *J. Cell. Physiol.* **215,** 434–441
23. Wall, D., Douglas, S., Ferro, V., Cowden, W., and Parish, C. (2001) *Thromb. Res.* **103,** 325–335
24. Olson, S. T., Björk, I., and Shore, J. D. (1993) *Methods Enzymol.* **222,** 525–559
25. Bock, P. E. (1992) *J. Biol. Chem.* **267,** 14963–14973
26. Dharmawardana, K. R., and Bock, P. E. (1998) *Biochemistry* **37,** 13143–13152
27. Bock, P. E. (1992) *J. Biol. Chem.* **267,** 14974–14981
28. Orcutt, S. J., and Krishnaswamy, S. (2004) *J. Biol. Chem.* **279,** 54927–54936
29. Fenton, J. W., 2nd, Fasco, M. J., and Stackrow, A. B. (1977) *J. Biol. Chem.* **252,** 3587–3598
30. Doyle, M. F., and Mann, K. G. (1990) *J. Biol. Chem.* **265,** 10693–10701
31. Mann, K. G., Elion, J., Butkowski, R. J., Downing, M., and Nesheim, M. E. (1981) *Methods Enzymol.* **80,** 286–302
32. Church, F. C., Meade, J. B., and Pratt, C. W. (1987) *Arch. Biochem. Biophys.* **259,** 331–340
33. Bock, P. E., Olson, S. T., and Björk, I. (1997) *J. Biol. Chem.* **272,** 19837–19845
34. Verhamme, I. M., Olson, S. T., Tollefsen, D. M., and Bock, P. E. (2002) *J. Biol. Chem.* **277,** 6788–6798
35. Meagher, J. L., Olson, S. T., and Gettins, P. G. (2000) *J. Biol. Chem.* **275,** 2698–2704
36. O'Keeffe, D., Olson, S. T., Gasiunas, N., Gallagher, J., Baglin, T. P., and Huntington, J. A. (2004) *J. Biol. Chem.* **279,** 50267–50273
37. Tian, W. X., and Tsou, C. L. (1982) *Biochemistry* **21,** 1028–1032
38. Hogg, P. J., and Jackson, C. M. (1989) *Proc. Natl. Acad. Sci. U.S.A.* **86,** 3619–3623
39. Lottenberg, R., Christensen, U., Jackson, C. M., and Coleman, P. L. (1981) *Methods Enzymol.* **80,** 341–361
40. Duggleby, R. G., and Morrison, J. F. (1977) *Biochim. Biophys. Acta* **481,** 297–312
41. Di Cera, E. (2008) *Mol. Aspects Med.* **29,** 203–254
42. Papaconstantinou, M. E., Gandhi, P. S., Chen, Z., Bah, A., and Di Cera, E. (2008) *Cell Mol. Life Sci.* **65,** 3688–3697
43. Craig, P. A., Olson, S. T., and Shore, J. D. (1989) *J. Biol. Chem.* **264,** 5452–5461
44. Olson, S. T., and Shore, J. D. (1986) *J. Biol. Chem.* **261,** 13151–13159
45. Johnson, K. A., Simpson, Z. B., and Blom, T. (2009) *Anal. Biochem.* **387,** 20–29
46. Johnson, K. A., Simpson, Z. B., and Blom, T. (2009) *Anal. Biochem.* **387,** 30–41
47. Turk, B., Brieditis, I., Bock, S. C., Olson, S. T., and Björk, I. (1997) *Biochemistry* **36,** 6682–6691
48. Buddai, S. K., Toulokhonova, L., Bergum, P. W., Vlasuk, G. P., and Krishnaswamy, S. (2002) *J. Biol. Chem.* **277,** 26689–26698
49. Dharmawardana, K. R., Olson, S. T., and Bock, P. E. (1999) *J. Biol. Chem.* **274,** 18635–18643
50. Tasset, D. M., Kubik, M. F., and Steiner, W. (1997) *J. Mol. Biol.* **272,** 688–698
51. Rand, M. D., Lock, J. B., van't Veer, C., Gaffney, D. P., and Mann, K. G. (1996) *Blood* **88,** 3432–3445
52. Hemker, H. C., Giesen, P., Al Dieri, R., Regnault, V., de Smedt, E., Wagenvoord, R., Lecompte, T., and Béguin, S. (2003) *Pathophysiol. Haemost. Thromb.* **33,** 4–15
53. Tchaikovski, S. N., VAN Vlijmen, B. J., Rosing, J., and Tans, G. (2007) *J. Thromb. Haemost.* **5,** 2079–2086
54. Desai, U. R., Petitou, M., Björk, I., and Olson, S. T. (1998) *J. Biol. Chem.* **273,** 7478–7487
55. Rezaie, A. R. (1998) *J. Biol. Chem.* **273,** 16824–16827
56. Gettins, P. G., and Olson, S. T. (2009) *J. Biol. Chem.* **284,** 20441–20445
57. Olson, S. T., Swanson, R., Raub-Segall, E., Bedsted, T., Sadri, M., Petitou, M., Hérault, J. P., Herbert, J. M., and Björk, I. (2004) *Thromb. Haemost.* **92,** 929–939
58. Streusand, V. J., Björk, I., Gettins, P. G., Petitou, M., and Olson, S. T. (1995) *J. Biol. Chem.* **270,** 9043–9051
59. Klauser, R. J., Meinetsberger, E., and Raake, W. (1991) *Semin. Thromb. Hemost.* **17,** Suppl. 1, 118–125
60. Klauser, R. J., Raake, W., Meinetsberger, E., and Zeiller, P. (1991) *J. Pharmacol. Exp. Ther.* **259,** 8–14
61. Raake, W., Klauser, R. J., Meinetsberger, E., Zeller, P., and Elling, H. (1991) *Semin. Thromb. Hemost.* **17,** Suppl. 1, 129–135
62. Ofosu, F. A., Fareed, J., Smith, L. M., Anvari, N., Hoppensteadt, D., and Blajchman, M. A. (1992) *Eur. J. Biochem.* **203,** 121–125
63. Béguin, S. S., Dol, F., and Hemker, H. C. (1991) *Semin. Thromb. Hemost.* **17,** Suppl. 1, 126–128
64. Böhme, C., Nimtz, M., Grabenhorst, E., Conradt, H. S., Strathmann, A., and Ragg, H. (2002) *Eur. J. Biochem.* **269,** 977–988
65. Kroh, H. K., Tans, G., Nicolaes, G. A., Rosing, J., and Bock, P. E. (2007) *J. Biol. Chem.* **282,** 16095–16104
66. Desai, U. R., Vlahov, I. R., Pervin, A., and Linhardt, R. J. (1995) *Carbohydr. Res.* **275,** 391–401
67. Zhu, X., Hsu, B. T., and Rees, D. C. (1993) *Structure* **1,** 27–34
68. Volkin, D. B., Verticelli, A. M., Marfia, K. E., Burke, C. J., Mach, H., and Middaugh, C. R. (1993) *Biochim. Biophys. Acta* **1203,** 18–26
69. Kulahin, N., Kiselyov, V., Kochoyan, A., Kristensen, O., Kastrup, J. S., Berezin, V., Bock, E., and Gajhede, M. (2008) *Acta Crystallogr. Sect. F Struct. Biol. Cryst. Commun.* **64,** 448–452
70. Yeh, B. K., Eliseenkova, A. V., Plotnikov, A. N., Green, D., Pinnell, J., Polat, T., Gritli-Linde, A., Linhardt, R. J., and Mohammadi, M. (2002) *Mol. Cell. Biol.* **22,** 7184–7192
71. Hung, K. W., Kumar, T. K., Kathir, K. M., Xu, P., Ni, F., Ji, H. H., Chen, M. C., Yang, C. C., Lin, F. P., Chiu, I. M., and Yu, C. (2005) *Biochemistry* **44,** 15787–15798
72. Innis, C. A., and Hyvönen, M. (2003) *J. Biol. Chem.* **278,** 39969–39977
73. Tollefsen, D. M. (1995) *Thromb. Haemost.* **74,** 1209–1214
74. Bock, P. E., Panizzi, P., and Verhamme, I. M. (2007) *J. Thromb. Haemost.* **5,** Suppl. 1, 81–94
75. Baglin, T. (2005) *Br. J. Haematol.* **130,** 653–661
76. Mammen, E. F. (1998) *Semin. Thromb. Hemost.* **24,** 19–25
77. He, L., Vicente, C. P., Westrick, R. J., Eitzman, D. T., and Tollefsen, D. M. (2002) *J. Clin. Invest.* **109,** 213–219
78. Noda, A., Wada, H., Kusiya, F., Sakakura, M., Onishi, K., Nakatani, K., Gabazza, E. C., Asahara, N., Tsukada, M., Nobori, T., and Shiku, H. (2002) *Clin. Appl. Thromb. Hemost.* **8,** 265–271
79. Kario, K., Matsuo, T., Kodama, K., Katayama, S., and Kobayashi, H. (1992) *Thromb. Res.* **66,** 435–444
80. Hiebert, L. M., Wice, S. M., Ping, T., Hileman, R. E., Polat, T., and Linhardt, R. J. (2002) *Pharm. Res.* **19,** 838–844